AMERICAN ACADEMY OF OPHTHALMOLOGY®

Utility of En Face OCT for the Detection of Clinically Unsuspected Retinal Neovascularization in Patients with Diabetic Retinopathy

Kotaro Tsuboi, MD,[1] *Mehdi Mazloumi, MD, MPH,*[1] *Yukun Guo, MS,*[1] *Jie Wang, PhD,*[1,2] *Christina J. Flaxel, MD,*[1] *Steven T. Bailey, MD,*[1] *David Huang, MD, PhD,*[1] *Yali Jia, PhD,*[1,2] *Thomas S. Hwang, MD*[1]

Purpose: To assess the value of en face OCT for detecting clinically unsuspected retinal neovascularization (RNV) in patients with nonproliferative diabetic retinopathy (NPDR).

Design: A retrospective, cross-sectional study.

Participants: Treatment-naïve patients clinically graded as NPDR in an ongoing prospective observational OCT angiography (OCTA) study at a tertiary care center.

Methods: Each patient underwent imaging of 1 eye with a spectral-domain OCTA, generating a 17 × 17-mm widefield image by montaging four 9 × 9-mm scans. Two independent graders examined a combination of en face OCT, en face OCTA with a custom vitreoretinal interface slab, and cross-sectional OCTA to determine the presence of RNV. We measured the area of RNV flow within RNV lesions on en face OCTA.

Main Outcome Measures: Detection rate of clinically occult RNV with OCT and OCTA.

Results: Of 63 enrolled eyes, 27 (43%) were clinically graded as severe NPDR, 16 (25%) as moderate NPDR, and 20 (32%) as mild NPDR. Using the combination of en face OCT, en face OCTA, and cross-sectional OCTA, the graders detected 42 RNV lesions in 12 (19%) eyes, of which 8 (67%) were graded as severe NPDR, 2 (17%) as moderate NPDR, and 2 (17%) as mild NPDR. The sensitivity of en face OCT alone for detecting eyes with RNV was similar to that of en face OCTA alone (100% vs. 92%; $P = 0.32$), whereas the specificity of en face OCT alone was significantly lower than that of en face OCTA alone (32% vs. 73%; $P < 0.001$). For detecting individual RNV lesions, the en face OCT was 100% sensitive, compared with 67% sensitivity for the en face OCTA ($P < 0.001$). The area of RNV lesions that manual grading with en face OCTA alone missed was significantly smaller than that of manually detectable RNV (Mean [standard deviation] RNV flow area, 0.015 [0.020] mm^2 vs. 0.16 [0.36] mm^2; $P < 0.001$).

Conclusion: The combination of en face OCT and OCTA can detect clinically occult RNV with high sensitivity. For screening these small lesions, en face OCT may be a useful imaging modality.

Financial Disclosure(s): Proprietary or commercial disclosure may be found after the references. *Ophthalmology Retina 2023;7:683-691 © 2023 by the American Academy of Ophthalmology*

Diabetic retinopathy (DR) is the leading cause of preventable blindness in the working middle-aged adult population, with a significant global burden that is expected to remain high through 2045.[1] Proliferative diabetic retinopathy (PDR) and diabetic macular edema (DME) are the two sight-threatening complications of DR and need to be promptly treated to prevent permanent vision loss in affected patients.[2] Although OCT has facilitated the objective diagnosis of DME, the early detection of PDR remains laborious for ophthalmologists, requiring a careful dilated fundus examination or fluorescein angiography (FA).[3] Small tufts of retinal neovascularization (RNV) can evade the examiner on fundus examination and can be difficult to distinguish from intraretinal microvascular abnormalities (IRMAs) or retinal hemorrhages. The widespread use of anti-VEGF agents for the treatment of DME has made the risk assessment for PDR more challenging, as anti-VEGF injections blunt the features of nonproliferative diabetic retinopathy (NPDR), while anti-VEGF therapy does not entirely prevent the progression to PDR.[4] When RNV lesions are present in this setting, they are frequently small and difficult to see.[5] This has made surveillance for early RNV lesions more challenging.

https://doi.org/10.1016/j.oret.2023.03.002
ISSN 2468-6530/23

The recent improvements in OCT angiography (OCTA) technology have made it possible not only to identify RNV based on the tissue plane above the internal limiting membrane (ILM) but to capture a wide field of view, making it a reasonable surveillance modality for RNV.[6–12] Our prior study demonstrated that widefield OCTA identified clinically unsuspected RNV in eyes with NPDR and that these RNV lesions were undetectable on color fundus photographs.[5] In addition to OCTA, a structural OCT can be a useful tool for distinguishing RNV from IRMA.[7,13–16] A combination of serial *en face* OCT and OCTA in branch retinal vein occlusion eyes demonstrated that hyperreflective tissue on *en face* OCT precedes a recognizable RNV lesion.[17] Recently, in a longitudinal study, we described the early stages of RNV on both *en face* OCT and *en face* OCTA in eyes with DR, and the early signs of RNV were more discernable using *en face* OCT.[18] Therefore, we speculated that the structural *en face* OCT might provide additional value for detecting RNV in eyes with DR.

To answer this question, we conducted a cross-sectional study to analyze the sensitivity and specificity of *en face* OCT and OCTA for the detection of clinically occult RNV in eyes clinically graded as NPDR. All RNV lesions were identified using a combination of en face OCT, en face OCTA with custom vitreoretinal interface (VRI) slab, and cross-sectional OCTA. The primary outcome measures were the detection rate of RNV on *en face* OCT vs. *en face* OCTA, the RNV membrane area on *en face* OCT, and the RNV flow area on *en face* OCTA.

Methods

We included patients from a prospective widefield OCTA study (NIH grant no.: R01 EY027833) performed at the Casey Eye Institute, Oregon Health Science University. The details of the studies have been previously published.[19–23] The study adhered to the tenets of the Declaration of Helsinki and complied the Health Insurance Portability and Accountability Act of 1996. The Institutional Review Board of Oregon Health Science University approved the study. Written informed consent was obtained from all the participants.

Study Participants

In a single-center cross-sectional study, we included consecutive adult patients with a diagnosis of NPDR of any severity based on fundus examination enrolled in the above described study between December 19, 2020 and February 15, 2022. We excluded patients with: (1) any previous treatment with intravitreal anti-VEGF or panretinal photocoagulation; (2) any other significant concomitant ocular disease; (3) any RNV seen on clinical examination or FA; (4) any previous retinal or glaucoma surgery; (5) myopia > -6 diopters; (6) vitreous hemorrhage or any other media opacities precluding adequate image acquisition; and (7) scans with a quality index of 5 or less or with artifacts that influenced the assessment. When both eyes of the patient met the eligibility criteria for the study, 1 eye was randomly selected for inclusion.

All patients underwent comprehensive ophthalmic examination, including the ETDRS (Precision vision) protocol visual acuity, slit-lamp biomicroscopy, intraocular pressure measurement, indirect stereoscopic fundus examination, and a commercial 120-kHz spectral-domain OCTA (Solix, Optovue) with 840-nm central wavelength.

Image Acquisition and Analysis

To avoid lowering the scan resolution to achieve widefield OCTA (approximately 17 × 17-mm), we montaged 4 high-resolution scans (600 × 600 sampling points over 9 × 9-mm) captured at superior temporal, superior nasal, inferior temporal, and inferior nasal quadrants.[24] To optimize the detection of RNV, we created 2 different custom slabs for *en face* OCT and *en face* OCTA based on our prior study.[18] The embedded software (version 2019 V1.0.1.1) generated the *en face* OCTA by projecting the angiographic signal from the ILM to 300 μm above the outer boundary of the ILM, which is commonly referred to as the VRI slab.[6,7,25,26] En face OCT was generated by projecting the structural OCT signal from the ILM to 30 μm above the ILM (Fig 1).

Masked from clinical information, 2 trained retina specialists (K.T. and M.M.) independently graded montaged *en face* OCT and OCTA for the presence of RNV by the commercial software. To generate the ground truth, the graders first identified foci of epiretinal hyperreflective material (EHM) on en face OCT or networks of vessels on *en face* OCTA as regions of interest.[27] Then, they examined the corresponding region on both imaging modalities and the cross-sectional OCTA (overlaid on OCT) (Fig 1). The lesion was determined to be RNV if a flow signal was present above the ILM on the cross-sectional OCTA. Then, we measured the sensitivity and specificity of *en face* OCT alone vs. *en face* OCTA alone for the detection of eyes with RNV, as well as individual RNV lesions against the ground truth.

We measured the membrane area and the flow area of each RNV lesion confirmed by the cross-sectional OCTA. Because a small RNV lesion was difficult to manually delineate on an en face image, the areas of membrane and flow were calculated using cross-sectional images. A series of cross-sectional OCTA (overlaid on OCT) images at the location of RNV lesions were generated using our custom software COOL-ART.[28,29] A third grader (G.Y.) manually segmented the RNV membrane defined as abnormal structures above the ILM, and the RNV flow defined as the abnormal flow signals breaching the ILM. After the RNV membrane and flow were segmented on all cross-sections through the entire scan volume, the 3-dimensional (3D) RNV membrane and RNV flow were constructed. We calculated the areas of the RNV membrane and the RNV flow by projecting 3D data into 2-dimensional maps.

Statistical Analysis

Statistical analysis was performed using SPSS software (version 25 for Windows, IBM). Continuous variables were expressed as mean and standard deviation (SD) of mean and categorical variables were expressed as n (%). One-sample Kolmogorov-Smirnov test was used to assess the normal distribution of variables in our sample. For variables without normal distribution, the logarithm transformation of the variable was entered in the analysis. Fisher exact test was used to compare the detection rate of RNV between widefield en face OCT and widefield-OCTA. To evaluate the intraobserver and interobserver reproducibility of measurements, 25 randomly selected scans from 25 eyes were evaluated. The analysis was based on 2 independent series of reevaluations made by 2 independent observers. The agreement between a single observer's measurements and the mean of the measurements by the 2 observers was calculated with the intraclass correlation coefficient (ICC) from a 2-way mixed-effect model. The comparisons between continuous and categorical variables of 2 paired groups (e.g., RNV

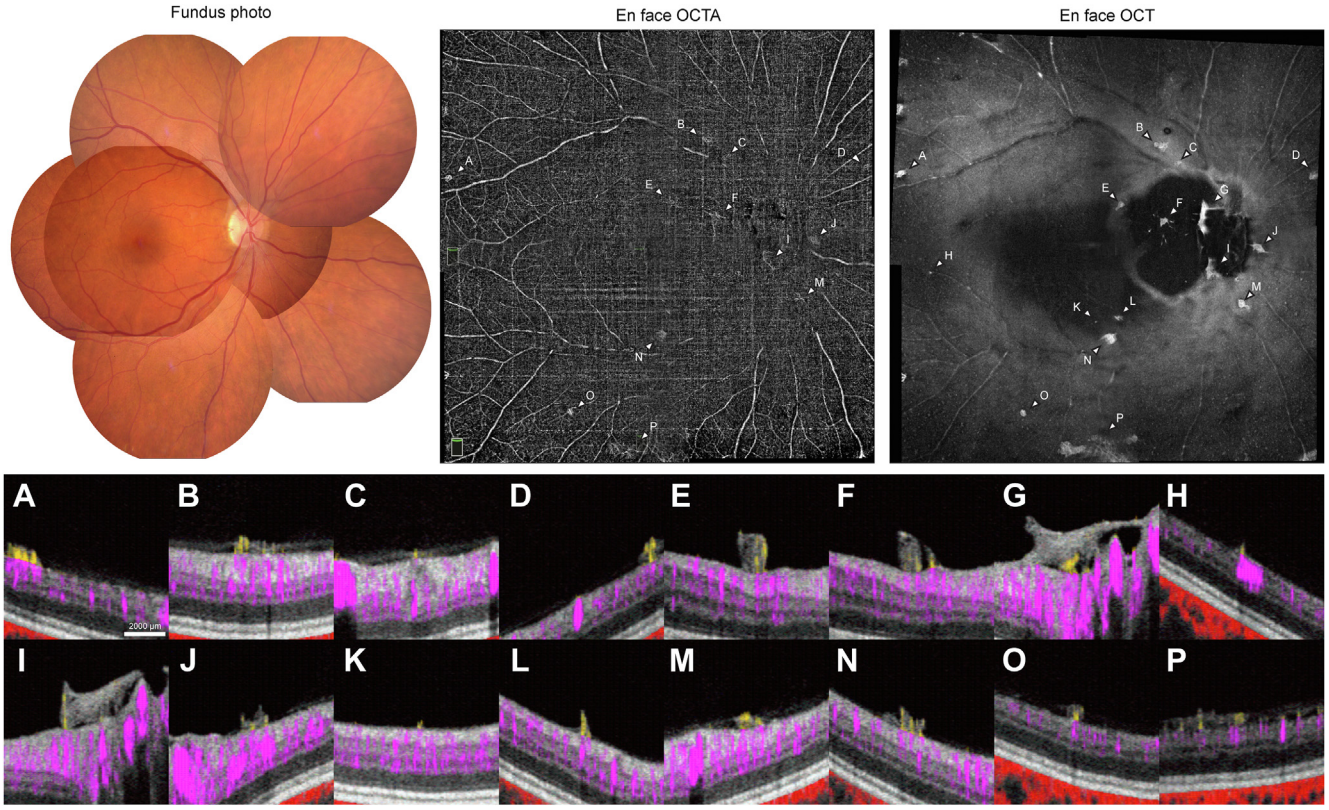

Figure 1. Detection of retinal neovascularization (RNV) in the unsuspected case using en face OCT and OCT angiography (OCTA). This eye is classified into moderate nonproliferative diabetic retinopathy based on the fundus photographs and clinical examinations. En face OCTA detected 12 abnormal areas of flow and en face OCT detected 16 foci of epiretinal hyperreflective material (EHM). Corresponding OCT B-scans with flow signals (**A**–**P**) show abnormal flows that breach the internal limiting membrane and extend into abnormal tissue on the retinal surface.

lesions detected by *en face* OCT vs. OCTA) were performed using the Wilcoxon signed-rank test and the McNemar test, respectively. A P value of < 0.05 was considered statistically significant.

Results

Sixty-three treatment-naïve eyes with NPDR from 63 patients were included in the study. Based on the clinical examination, 27 (43%) of the eyes were graded as severe NPDR, 16 (25%) as moderate NPDR, and 20 (32%) as mild NPDR. The mean (SD) age was 61.0 (11.7), and 30 (48%) patients were women. The mean (SD) BCVA was 77 (8) letters. The interobserver reliability for the presence of RNV on *en face* OCT and OCTA had an ICC of 0.889 and 0.996, respectively.

The 2 graders confirmed the presence of 42 clinically occult RNV lesions in 12 (19%) eyes using a combination of *en face* OCT, *en face* OCTA, and cross-sectional OCTA. Of these 12 eyes, 8 (67%) were graded as severe NPDR, 2 (17%) as moderate NPDR, and 2 (17%) as mild NPDR. Eleven eyes had only neovascularization elsewhere, and only 1 eye had neovascularization of the disc and neovascularization elsewhere. Clinically occult RNV lesions were detected by the combination of *en face* OCT, *en face*. OCTA, and cross-sectional OCT with flow. They can appear like retinal hemorrhages or IRMAs, while some of these lesions were sometimes without corresponding pathology on color fundus photograph (Fig 2). Overall, the mean (SD) membrane area of an RNV lesion on en face OCT (0.12 [0.30] mm^2, [95% confidence interval {CI}, 0.026–0.21]) was larger than the mean flow area by en face OCTA (0.027 [0.029] mm^2, [95% CI, 0.018–0.036]; $P < 0.001$ by Wilcoxon signed-rank test) by a factor (SD) of 3.4 (2.8) (95% CI, 2.5–4.3 times) (Fig 3).

The sensitivity of *en face* OCT for detecting eyes with RNV was similar to that of *en face* OCTA (100% vs. 92%; $P = 0.32$ by the McNemar test), whereas the specificity of *en face* OCT was significantly lower than that of *en face* OCTA (32% vs. 73%; $P < 0.001$). At the level of the individual RNV lesion, the en face OCT was 100% sensitive, compared with 67% sensitivity for the *en face* OCTA ($P < 0.001$). Comparing the area of RNV flow of the 14 RNV lesions that graders missed with *en face* OCTA alone to grader-detected RNV, the area of RNV lesions missed by graders was significantly smaller than that of manually detectable RNV (mean [SD] RNV flow area, 0.015 [0.020] mm^2 [95% CI, 0.0034–0.026] vs. 0.16 [0.36] mm^2 [95% CI, 0.012–0.30], $P < 0.001$ by Mann–Whitney U test).

Both *en face* OCT and *en face* OCTA had artifacts that led to false-positive detection of RNV. On *en face* OCT, vessel crossings were frequently misidentified as EHM. Figure 4 demonstrates 3 distinct hyperreflective foci on en face OCT, but one of the lesions (Fig 4C) is a vessel crossing without a flow signal above

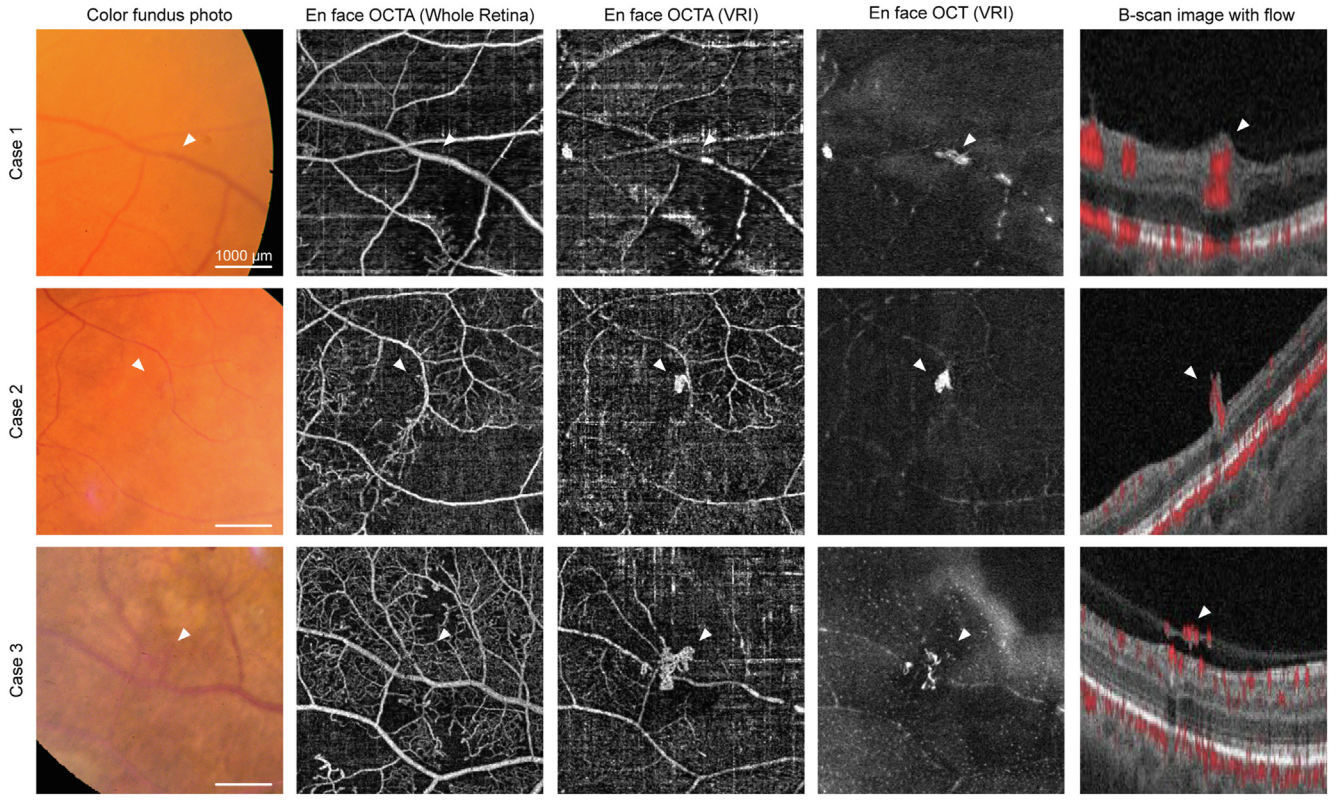

Figure 2. Clinically occult retinal neovascularization (RNV) on color fundus photograph. (Top row, case 1) On the color fundus photograph, there are no abnormalities (white arrow). *En face* OCT with vitreoretinal interface (VRI) slab illustrates a small RNV and flow signal breaching the internal limiting membrane (ILM) confirmed by a B-scan image with flow signal. (Middle row, case 2) A retinal hemorrhage (white arrow) is indicated on the color fundus photograph. A forward RNV is visualized at the location of the retinal hemorrhage by *en face* OCT and *en face* OCTA. (Bottom row, case 3) A tabletop RNV is identified on *en face* OCT and *en face* OCTA at the location of intraretinal microvascular abnormalities on the color fundus photo. Scale bar = 1000 μm.

the ILM on cross-sectional OCTA. In the same scan, *en face* OCTA shows a different artifact (red arrows) where a flow signal above the ILM is present without expected abnormal tissue for RNV (Fig 4D). These ghost flow signals are frequently seen at the location of hyperreflective pixels and are presumably caused by saturation artifacts, which is a well-known artifact in OCT that occurs when the received signal exceeds the dynamic range of the spectrometer.[30–32]

Discussion

In this study, we found that *en face* OCT is valuable for detecting unsuspected RNV in eyes clinically graded as NPDR. OCT angiography allows noninvasive detection of RNV,[6,7] and with a wider field of view, it can potentially be useful for routine surveillance of RNV in DR patients.[5] Studies have previously demonstrated the value of structural OCT for detecting RNV.[7,11,13,14,17,18] Because a single OCTA scan can generate both *en face* OCT and *en face* OCTA simultaneously, combining these 2 imaging modalities may be an efficient method for screening for RNV. For detecting individual RNV lesions, the *en face* OCT alone was significantly more sensitive than the *en face* OCTA because the area of the RNV membrane detected by *en face* OCT was larger than the area of RNV flow on *en face* OCTA. Thus, *en face* OCT may be a valuable tool for the initial screening of small RNVs in eyes with DR.

In the current study, *en face* OCT and *en face* OCTA had high sensitivities for both detecting eyes with RNV (100% and 92%, respectively) and for detecting individual RNV lesions (100% and 67%, respectively). A prior study by Hirano et al[6] demonstrated that the sensitivity of en face OCTA for identifying RNV found on FA was 73%. Lu et al[11] have reported that the combination of *en face* OCT and *en face* OCTA improved the detection rate of individual RNV lesions, but the sensitivity of en face OCTA was higher than that of en face OCT. The VRI slab for *en face* OCT in their study was thicker than that our slab, and this difference may partly explain the discrepancy. Additionally, these studies used swept-source OCTA to identify RNV in eyes with known PDR, whereas we used spectral-domain OCTA for detecting RNV in eyes graded as NPDR, which may also contribute to the difference.

A combination of *en face* OCT and OCTA detected subclinical RNV in approximately a fifth of eyes graded as

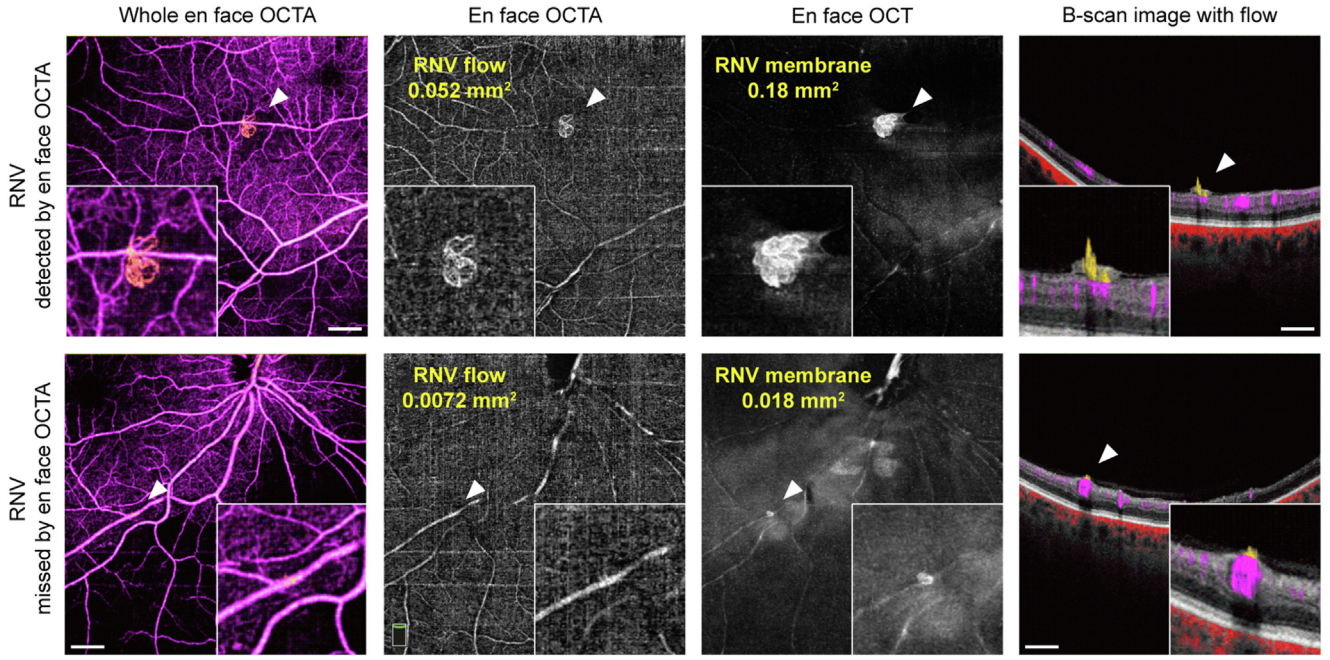

Figure 3. Detected and missed retinal neovascularization (RNV) using en face OCT angiography (OCTA) alone. In the detected RNV, abnormal flow and tissue are illustrated by both *en face* OCTA and OCT. In the missed RNV, *en face* OCT visualizes the abnormal tissue, while the abnormal flow is barely detected. Scale bar = 1000 μm.

NPDR that were barely detectable on color fundus photograph (Fig 2). Although clinical gradings have been prospectively validated in assessing risk of vision loss and progression to clinically evident PDR, this study provides evidence that clinical examinations miss important pathologic lesions in a significant portion of patients. In fact, ETDRS reported that a nontrivial percentage of patients with mild-to-moderate NPDR progressed to PDR in one year, ranging from 4.5% for level 35 to 26.0% for level 47.[33] In our study, the NPDR cohort had unsuspected RNV lesions in 10% to 30% of patients, with more severe levels having a higher percentage of eyes with RNV. The current study was not designed to demonstrate the clinical significance of the subclinical RNV lesions. We hypothesize that if RNV develops first through a subclinical stage like the ones found in this study, it may mean that the identification of subclinical RNV may be a more sensitive way to predict the short-term risk of progression to clinically evident PDR compared with photographic grading. By identifying precursors of RNV rather than relying on indirect features of the retina, such as intraretinal hemorrhages to predict the risk of progression, we may be able to more precisely identify eyes at risk of developing PDR in the short term. A further longitudinal study is needed to clarify this question.

This study is limited by the relatively small field of view. Although prior studies demonstrated a high sensitivity (73%−100%) for identifying the eyes with RNV using OCTA imaging,[8,9,12] a single 12 × 12-mm OCTA and a 15 × 9-mm montaged OCTA are expected to detect only approximately 40% of individual RNV lesions detected by ultra-widefield FA.[9,10] An ultra-widefield OCTA, constructed by merging five 12 × 12-mm OCTA scans, may be necessary to detect 80% of lesions.[9] The field of view in this study is only 17 × 17 mm, smaller than the field covered by the ETDRS 7 fields and much smaller than ultra-widefield fundus photography available today. Even this view is generated with a montage technique, which requires eccentric fixation and excellent cooperation by the patient. The acquisition takes time and a skilled operator. Further advances in hardware are required to improve the field of view and acquisition efficiency without sacrificing the resolution and quality of images.

Another drawback of this approach is that neither *en face* OCT nor OCTA was highly specific for RNV when used individually. The most frequent reasons for false-positive detection of RNV were vessel crossings on *en face* OCT and ghost flow signals on *en face* OCTA, presumably caused by saturation artifacts.[30−32] These saturated spectrum spikes are unstable, and tiny variations between consecutive B-scans in the same position can generate a strong OCTA signal (Fig 4D). Therefore, examining the cross-sectional OCTA (overlaid on OCT) was necessary to determine whether the hyperreflective material on OCT or the flow signal of OCTA in the slab above the ILM truly represented RNV. And because a widefield OCTA has many B-scans (2400 for a 17 × 17-mm scan in this study), this may be impractical for everyday use. It is possible, however, that an automated algorithm could be trained with enough examples to recognize false-positive lesions to improve the specificity of these modalities for the detection of RNV.

Also, it is not clear from this study whether *en face* OCT or OCTA would be optimal for detection of the subclinical RNV lesions. *En face* OCT had a higher sensitivity but

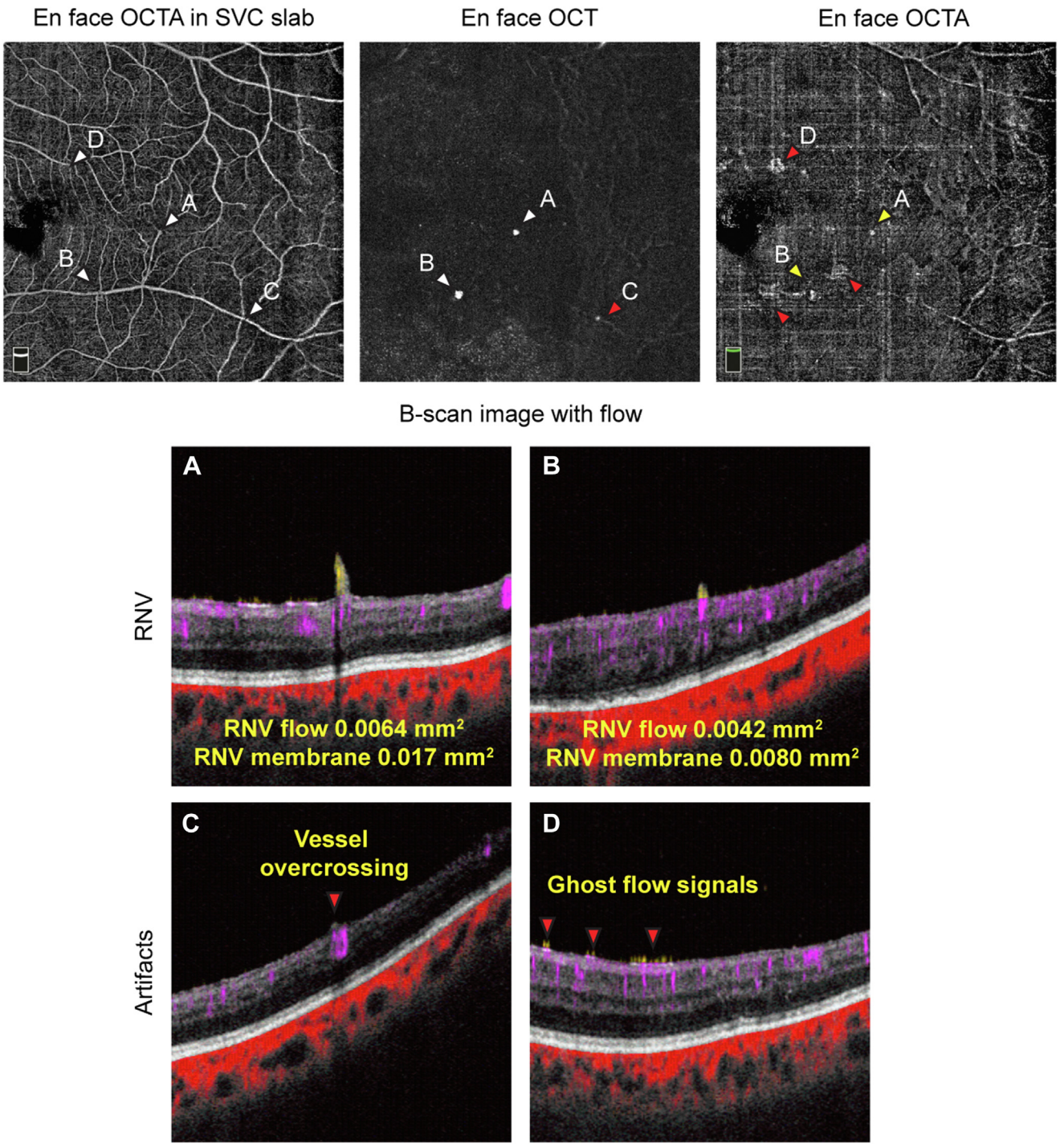

Figure 4. A moderate NPDR eye with 2 retinal neovascularization (RNV). On *en face* OCT, 2 of the hyperreflective foci corresponded to RNV and one corresponded to a vessel crossing (red arrow). On *en face* OCTA, 2 RNVs were missed (yellow arrows), and 3 abnormal flow signals were incorrectly diagnosed as RNV suspected (red arrows). OCT B-scans with flow overlaid show abnormal flow signals breach into the vitreous cavity with abnormal tissue (**A**, **B**). Vessel over-crossing sites are common artifacts on *en face* OCT (**C**), and ghost flow signals above the hyperreflective tissue without abnormal tissues are common on *en face* OCTA (**D**).

lower specificity for detecting eyes with RNV compared with *en face* OCTA. In developing an automated algorithm for detection of RNV, one could optimize the diagnostic performance by setting the optimal threshold for the area or applying filters that select for vessels.

This study had several limitations. First, FA was not available for every case, which could have served as another reference point to evaluate the efficacy of widefield en face OCT and en face OCTA in detection of RNV. However, Lee et al[13] have demonstrated that lesions that are clearly

neovascular in nature based on tissue planes do not always have the characteristic leakage on FA. Although FA would have provided an alternate point of reference for these lesions, it may not be a reliable ground truth for RNV lesions. Second, the eyes with NPDR were initially graded based on the 7-field fundus photograph; however, 21 (33%) eyes did not have the fundus photograph at the date when we obtained the widefield OCTA imaging and we graded them based on the previous fundus photograph and clinical examinations at the time of OCTA imaging. Third, because of the cross-sectional design of our study, we were not able to follow the natural course of the small RNV detected in our cohort. As Schwartz et al[7] mentioned in the prior study, structural OCT should not be used to follow RNV lesions, because it does not detect regression of flow signal. Similarly, it is likely that en face OCT alone cannot reliably demonstrate regression. A longitudinal study that looks at the evolution of these lesions, especially those undergoing treatment, is necessary to elucidate this. Finally, it is unclear if the very small *en face* OCT-detected RNV lesions are clinically significant and if their detection and early treatment could meaningfully reduce the risk of vision loss.

In conclusion, both *en face* OCT and *en face* OCTA demonstrate small clinically unsuspected RNV lesions in the VRI slab of eyes graded as NPDR. *En face* OCT was more sensitive than *en face* OCTA, and the RNV membrane area measured on *en face* OCT was significantly larger than the area of RNV flows measured on *en face* OCTA. Although the detection flow signal breaching the ILM with cross-sectional OCTA was essential in confirming the nature of the lesions, *en face* OCT may be a useful screening method for detecting unsuspected RNV lesions in eyes DR.

Acknowledgments

The authors thank Ms. Elizabeth White, a statistician, for her advice.

Footnotes and Disclosures

Originally received: December 6, 2022.
Final revision: February 28, 2023.
Accepted: March 7, 2023.
Available online: March 12, 2023. Manuscript no. ORET-D-22-00758R11

[1] Department of Ophthalmology, Casey Eye Institute, Oregon Health & Science University, Portland, Oregon.

[2] Department of Biomedical Engineering, Oregon Health & Science University, Portland, Oregon.

Disclosure(s):

All authors have completed and submitted the ICMJE disclosures form.

The authors made the following disclosures: D.H.: Grants − Optovue Inc; Royalties − Optovue Inc; Consultant − Optovue Inc; Payment for expert testimony − Optovue Inc.

K.T.: Honoraria − Bayer, Chugai, Santen.

S.T.B.: Consultant − Optovue Inc.

Y.J.: Patents planned issues or pending − Optovue Inc, Optos Inc.

The other author(s) have no proprietary or commercial interest in any materials discussed in this article.

Oregon Health & Science University (OHSU) has significant financial interest in Optovue Inc, a company that may have a commercial interest in the results of this research and technology. These potential conflicts of interest have been reviewed and managed by OHSU.

Supported by the National Institute of Health (grant no.: R01 EY027833, R01 EY024544, T32 EY023211, UL1TR002369, and P30 EY010572), an Unrestricted Departmental Funding Grant, the Dr. H. James and Carole Free Catalyst Award from Research to Prevent Blindness (New York, NY), and the Bright Focus Foundation (grant no.: G2020168). The funding source had no role in the design and conduct of the study; collection, management, analysis, and interpretation of the data; preparation, review, or approval of the manuscript; and decision to submit the manuscript for publication.

HUMAN SUBJECTS: This study adhered to the tenets of the Declaration of Helsinki and complied with the Health Insurance Portability and Accountability Act of 1996. The Institutional Review Board of Oregon Health Science University approved the study. Written informed consent was obtained from all the participants.

No animals were used in this study.

Author Contributions:

Conception and Design: Tsuboi, Mazloumi, Hwang

Data Collection: Tsuboi, Mazloumi, Flaxel, Bailey, Huang, Hwang

Analysis and Interpretation: Tsuboi, Mazloumi, Guo, Wang, Huang, Jia, Hwang

Obtained Funding: Jia, Hwang

Overall Responsibility: Tsuboi, Mazloumi, Huang, Jia, Hwang

Abbreviations and Acronyms:
CI = confidence interval; **DM** = diabetes mellitus; **DME** = diabetic macular edema; **DR** = diabetic retinopathy; **EHM** = epiretinal hyperreflective material; **ICC** = interclass correlation coefficient; **ILM** = internal limiting membrane; **IRMA** = intraretinal microvascular abnormality; **NPDR** = nonproliferative diabetic retinopathy; **OCTA** = OCT angiography; **PDR** = proliferative diabetic retinopathy; **RNV** = retinal neovascularization; **SD** = standard deviation; **VRI** = vitreoretinal interface; **3D** = 3-dimensional.

Keywords:
Diabetic Retinopathy, En face OCT, OCT Angiography, Retinal Neovascularization.

Correspondence:
Thomas Hwang, MD, Casey Eye Institute, Oregon Health & Science University, 515 SW Campus Dr, Portland, OR 97239. E-mail: hwangt@ohsu.edu.

References

1. Teo ZL, Tham YC, Yu M, et al. Global prevalence of diabetic retinopathy and projection of burden through 2045: systematic review and meta-analysis. *Ophthalmology*. 2021;128(11):1580−1591.
2. Cheung N, Mitchell P, Wong TY. Diabetic retinopathy. *Lancet*. 2010;376(9735):124−136.
3. Pearce E, Sivaprasad S. A review of advancements and evidence gaps in diabetic retinopathy screening models. *Clin Ophthalmol*. 2020;14:3285−3296.
4. Ip MS, Domalpally A, Sun JK, Ehrlich JS. Long-term effects of therapy with ranibizumab on diabetic retinopathy severity and baseline risk factors for worsening retinopathy. *Ophthalmology*. 2015;122(2):367−374.
5. You QS, Guo Y, Wang J, et al. Detection of clinically unsuspected retinal neovascularization with wide-field optical coherence tomography angiography. *Retina*. 2020;40(5):891−897.
6. Hirano T, Hoshiyama K, Hirabayashi K, et al. Vitreoretinal interface slab in OCT angiography for detecting diabetic retinal neovascularization. *Ophthalmol Retina*. 2020;4(6):588−594.
7. Schwartz R, Khalid H, Sivaprasad S, et al. Objective evaluation of proliferative diabetic retinopathy using OCT. *Ophthalmol Retina*. 2020;4(2):164−174.
8. Sawada O, Ichiyama Y, Obata S, et al. Comparison between wide-angle OCT angiography and ultra-wide field fluorescein angiography for detecting non-perfusion areas and retinal neovascularization in eyes with diabetic retinopathy. *Graefes Arch Clin Exp Ophthalmol*. 2018;256(7):1275−1280.
9. Russell JF, Flynn Jr HW, Sridhar J, et al. Distribution of diabetic neovascularization on ultra-widefield fluorescein angiography and on simulated widefield OCT angiography. *Am J Ophthalmol*. 2019;207:110−120.
10. Zhu Y, Cui Y, Wang JC, et al. Different scan protocols affect the detection rates of diabetic retinopathy lesions by wide-field swept-source optical coherence tomography angiography. *Am J Ophthalmol*. 2020;215:72−80.
11. Lu ES, Cui Y, Le R, et al. Detection of neovascularisation in the vitreoretinal interface slab using widefield swept-source optical coherence tomography angiography in diabetic retinopathy. *Br J Ophthalmol*. 2022;106(4):534−539.
12. Cui Y, Zhu Y, Wang JC, et al. Comparison of widefield swept-source optical coherence tomography angiography with ultra-widefield colour fundus photography and fluorescein angiography for detection of lesions in diabetic retinopathy. *Br J Ophthalmol*. 2021;105(4):577−581.
13. Lee CS, Lee AY, Sim DA, et al. Reevaluating the definition of intraretinal microvascular abnormalities and neovascularization elsewhere in diabetic retinopathy using optical coherence tomography and fluorescein angiography. *Am J Ophthalmol*. 2015;159(1):101, 10.e1.
14. Vaz-Pereira S, Silva JJ, Freund KB, Engelbert M. Optical coherence tomography angiography features of neovascularization in proliferative diabetic retinopathy. *Clin Ophthalmol*. 2020;14:3351−3362.
15. Arya M, Sorour O, Chaudhri J, et al. Distinguishing intraretinal microvascular abnormalities from retinal neovascularization using optical coherence tomography angiography. *Retina*. 2020;40(9):1686−1695.
16. Russell JF, Shi Y, Hinkle JW, et al. Longitudinal wide-field swept-source OCT angiography of neovascularization in proliferative diabetic retinopathy after panretinal photocoagulation. *Ophthalmol Retina*. 2019;3(4):350−361.
17. Tsuboi K, Ishida Y, Wakabayashi T, Kamei M. Presumed glial sprouts as a predictor of preretinal neovascularization in retinal vein occlusion. *JAMA Ophthalmol*. 2022;140(3):284−285.
18. Tsuboi K, Mazloumi M, Guo Y, et al. *Early sign of retinal neovascularization evolution in diabetic retinopathy: a longitudinal optical coherence tomography angiography study*. 2021. In press.
19. Hwang TS, Zhang M, Bhavsar K, et al. Visualization of 3 distinct retinal plexuses by projection-resolved optical coherence tomography angiography in diabetic retinopathy. *JAMA Ophthalmol*. 2016;134(12):1411−1419.
20. You QS, Wang J, Guo Y, et al. Optical coherence tomography angiography avascular area association with 1-year treatment requirement and disease progression in diabetic retinopathy. *Am J Ophthalmol*. 2020;217:268−277.
21. You QS, Wang J, Guo Y, et al. Detection of reduced retinal vessel density in eyes with geographic atrophy secondary to age-related macular degeneration using projection-resolved optical coherence tomography angiography. *Am J Ophthalmol*. 2020;209:206−212.
22. You QS, Tsuboi K, Guo Y, et al. Comparison of central macular fluid volume with central subfield thickness in patients with diabetic macular edema using optical coherence tomography angiography. *JAMA Ophthalmol*. 2021;139(7):734−741.
23. Tsuboi K, You QS, Guo Y, et al. Association between fluid volume in inner nuclear layer and visual acuity in diabetic macular edema. *Am J Ophthalmol*. 2022;237:164−172.
24. Wang J, Camino A, Hua X, et al. Invariant features-based automated registration and montage for wide-field OCT angiography. *Biomed Opt Express*. 2018;10(1):120−136.
25. Shiraki A, Sakimoto S, Eguchi M, et al. Analysis of progressive neovascularization in diabetic retinopathy using widefield OCT angiography. *Ophthalmol Retina*. 2022;6(2):153−160.
26. Cui Y, Zhu Y, Lu ES, et al. Widefield swept-source OCT angiography metrics associated with the development of diabetic vitreous hemorrhage: a prospective study. *Ophthalmology*. 2021;128(9):1312−1324.
27. Munk MR, Kashani AH, Tadayoni R, et al. Standardization of OCT angiography nomenclature in retinal vascular diseases: first survey results. *Ophthalmol Retina*. 2021;5(10):981−990.
28. Zhang M, Wang J, Pechauer AD, et al. Advanced image processing for optical coherence tomographic angiography of macular diseases. *Biomed Opt Express*. 2015;6(12):4661−4675.
29. Guo Y, Camino A, Zhang M, et al. Automated segmentation of retinal layer boundaries and capillary plexuses in wide-field optical coherence tomographic angiography. *Biomed Opt Express*. 2018;9(9):4429−4442.

30. Asrani S, Sarunic M, Santiago C, Izatt J. Detailed visualization of the anterior segment using fourier-domain optical coherence tomography. *Arch Ophthalmol*. 2008;126(6):765–771.
31. Li X, Liang S, Zhang J. Suppression of saturation artifacts in swept source optical coherence tomography using dual channel detection. *Proc Spie*. 2016:96972P, 96972P–6.
32. Liu H, Cao S, Ling Y, Gan Y. Inpainting for saturation artifacts in optical coherence tomography using dictionary-based sparese representation. *IEEE Photonics J*. 2021;13(2):3900110.
33. Fundus photographic risk factors for progression of diabetic retinopathy. ETDRS report number 12. Early Treatment Diabetic Retinopathy Study Research Group. *Ophthalmology*. 1991;98(Suppl 5):823–833.

Pictures & Perspectives

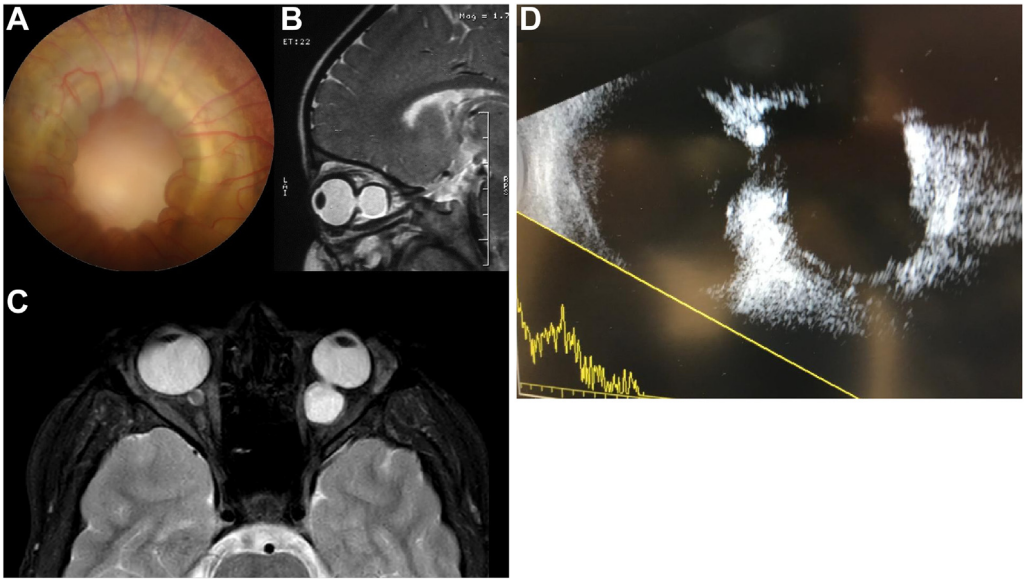

A Huge Posterior Staphyloma

A 10-year-old girl was referred for decreased vision in addition to exotropia in the left eye. The girl was healthy and had an unremarkable birth and family history. The patient's systemic examination, including neurologic assessment, was within normal limits.Fundus examination of the left eye revealed a deep excavation in the posterior wall, and the optic disc was not visible (**A**). The sagittal magnetic resonance image demonstrated excavation in the posterior wall of the globe in the left orbit (**B**). The axial magnetic resonance T2-weighted lipid-suppressed image of the left orbit exhibited continuity of the excavation in the posterior wall of the globe and vitreous cavity (**C**). A B-mode ultrasonography image showed that the size of the excavation was almost equal to that of the globe (**D**). (Magnified version of Figure **A**-**D** is available online at www.ophthalmologyretina.org)

Kemal Tekin, MD
Mehmet Yasin Teke, MD
Ulucanlar Eye Training and Research Hospital, Ophthalmology Department, Ankara, Turkey